

# REDUCING ORBITAL ECCENTRICITY IN BINARY BLACK HOLE SIMULATIONS

HARALD P. PFEIFFER<sup>1</sup>, DUNCAN A. BROWN<sup>1,2</sup>, LAWRENCE E. KIDDER<sup>3</sup>,  
LEE LINDBLOM<sup>1</sup>, GEOFFREY LOVELACE<sup>1</sup> and MARK A. SCHEEL<sup>1</sup>

<sup>1</sup>*Theoretical Astrophysics, California Institute of Technology, Pasadena, California 91125*

<sup>2</sup>*LIGO Laboratory, California Institute of Technology, Pasadena, California 91125*

<sup>3</sup>*Center for Radiophysics and Space Research, Cornell University, Ithaca, New York, 14853*

Binary black hole simulations starting from quasi-circular (*i.e.*, zero radial velocity) initial data have orbits with small but non-zero orbital eccentricities. Nonzero radial velocities are added to the quasi-equilibrium formalism for constructing binary black hole initial data, and it is demonstrated how the orbital frequency and radial velocities can be tuned to obtain inspiral trajectories with significantly reduced orbital eccentricity.

## 1. Introduction

The orbits of inspiraling compact objects such as black holes circularize during the inspiral due to the emission of gravitational waves,<sup>1</sup> so that binaries formed from stellar evolution (rather than dynamical capture) are expected to have very small eccentricities as they approach merger. For this reason and because the inspiral timescale is much longer than the orbital timescale, the assumption of a quasi-circular orbit (*i.e.*, zero radial velocities) has been widely used in the construction of binary black hole initial data.<sup>2-6</sup> Inspiral compact objects must, however, have a small inward radial velocities. Neglecting these radial velocities in the initial data leads to eccentricity in the subsequent evolution, as found here and in Refs. 7,8. It is therefore necessary to devise a formalism for constructing initial data that allows radial velocities on the individual black holes to be specified.

## 2. Binary black hole initial data with nonzero radial velocities

Incorporating radial velocities in puncture initial data<sup>9</sup> is straightforward because the full linear momentum of each hole can be specified. For quasi-equilibrium initial data<sup>4-6</sup> this is more difficult, because the assumption of quasi-circularity is fundamentally tied to a corotating coordinate system. However, we have shown<sup>8</sup> that corotating coordinates are not central to the scheme and identical initial data can be obtained in an asymptotically inertial coordinate system: one merely requires that the black holes move on circular coordinate trajectories rather than remaining fixed. This idea can be generalized by requiring that the black holes move on inspiral trajectories.<sup>8</sup> For corotating black holes, this is accomplished by adopting the following shift boundary condition on each of the black hole excision surfaces:

$$\beta^i = \alpha s^i - (\Omega_0 \times \mathbf{r})^i + v_r \frac{r^i}{r_0}. \quad (1)$$

Here  $\alpha$  is the lapse,  $s^i$  the outward-pointing spatial unit normal to the excision surface, and  $r_0$  is the coordinate distance between the center of the excision surface and the origin. The term  $(\Omega_0 \times \mathbf{r})^i$  causes the horizons to rotate about the origin

with orbital frequency  $\Omega_0$ ; the last term in Eq. (1) encodes the radial velocity  $v_r$  of the black hole with respect to the origin. Besides Eq. (1), the only other change to the standard quasi-equilibrium equations of Refs. 5,6 appears in the outer shift boundary condition, which becomes  $\beta^i \rightarrow 0$  as  $r \rightarrow \infty$ . A non-zero radial velocity is consistent with the horizon being in quasi-equilibrium, and does not prevent the addition of any desired spin on the black holes.<sup>8</sup>

### 3. Choice of orbital frequency and radial velocity

To demonstrate the orbital eccentricity of quasi-circular initial data, we construct such data for corotating black holes (coordinate separation  $d = 20$  of Table IV in Ref. 5;  $M_{\text{ADM}}\Omega_0 = 0.029792$ ,  $v_r = 0$ ) and evolve it for about 5 orbits with the computational methods of Refs. 10–12. The dotted line on the left panel of Fig. 1 is  $ds(t)/dt$ , where  $s(t)$  is the proper separation between the apparent horizons along the coordinate line connecting the centers of the holes. This quantity clearly exhibits oscillatory behavior due to the orbital eccentricity of the binary.

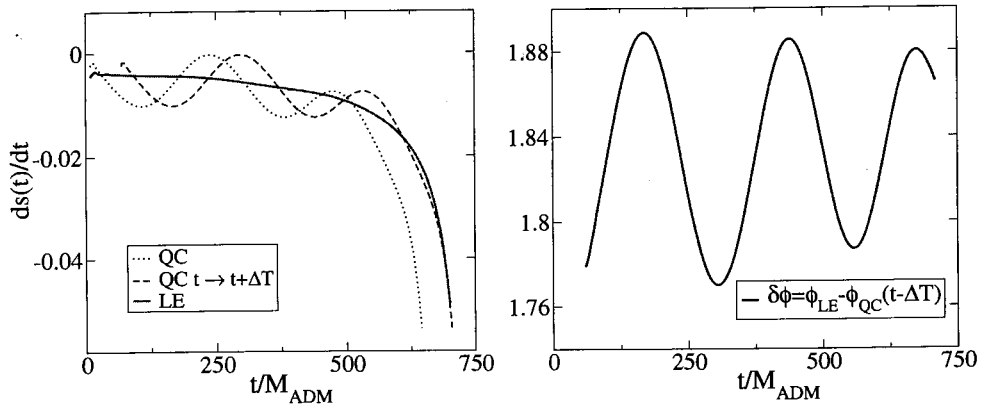


Fig. 1. Left: Radial velocity for evolutions of quasi-circular (QC; dotted line) and low-eccentricity (LE; solid line) initial data. The dashed line results from time-shifting the quasi-circular run by  $\Delta T$ . Right: Difference in orbital phase between LE and time-shifted QC.

In Newtonian gravity,  $\Omega_0$  and  $v_r$  influence the orbit in a straightforward way:  $v_r$  is the initial radial velocity, and  $\Omega_0$  is related to the initial radial acceleration, i.e. increasing  $\Omega_0$  makes  $d^2s/dt^2$  larger. This correspondence also holds approximately for binary black holes. Given initial guesses for  $\Omega_0$  and  $v_r$ , we construct initial data and evolve these data to produce a plot of  $ds/dt$  versus time. We then proceed iteratively, computing the next guesses for  $\Omega_0$  and  $v_r$  to reduce the oscillations in  $ds/dt$ . For the results presented here, we adjusted either  $\Omega_0$  or  $v_r$  in each iteration, starting from a simple guess in the first iteration and subsequently using linear interpolation between the previous iterations. We obtain the final parameters  $\Omega_0 = 0.029963/M_{\text{ADM}}$  and  $v_r = -0.0015$ , resulting in the evolution shown by the solid

line in the left panel of Fig. 1, which has barely discernible oscillations.

The black holes appear to approach each other more quickly and merge earlier in the evolution of the quasi-circular initial data. This corresponds to a simple coordinate time shift  $t \rightarrow t + \Delta T$  with  $\Delta T = 59M_{\text{ADM}}$  to the quasi-circular evolution, resulting in the dashed curve in Fig. 1. This curve now oscillates around the low-eccentricity curve, with no discernible secular drift. The right panel of Fig. 1 presents the orbital phase difference  $\delta\phi$  between the low-eccentricity run and the (time-shifted) quasi-circular run. The offset of  $\delta\phi$  from zero corresponds to the orbital phase acquired by the low-eccentricity run up to  $t = \Delta T$ ;  $\delta\phi$  oscillates around its mean without a noticeable secular drift.

A more comprehensive analysis of these evolutions<sup>8</sup> confirms the trends seen here using a variety of additional diagnostics, like orbital phase and frequency, and phase and frequency of gravitational waves. Because no coherent phase difference builds up, this more comprehensive study also demonstrates very high overlaps between gravitational waveforms from quasi-circular and low-eccentricity evolutions.

## Acknowledgments

We thank Gregory Cook for inspiring discussions. This work was supported in part by grants from the Sherman Fairchild Foundation and from the Brinson Foundation; by NSF grants PHY-0099568, PHY-0244906, PHY-0601459, DMS-0553302 and NASA grants NAG5-12834, NNG05GG52G at Caltech; and by NSF grants PHY-0312072, PHY-0354631, and NASA grant NNG05GG51G at Cornell. Some of the simulations discussed here were produced with LIGO Laboratory computing facilities. LIGO was constructed by Caltech and MIT with funding from the NSF and operates under cooperative agreement PHY-0107417.

## References

1. P. C. Peters, *Phys. Rev.* **136**, B1224(Nov 1964).
2. E.ourgoulhon, P. Grandclément and S. Bonazzola, *Phys. Rev. D* **65**, 044020 (2002).
3. P. Grandclément, E.ourgoulhon and S. Bonazzola, *Phys. Rev. D* **65**, 044021 (2002).
4. G. B. Cook, *Phys. Rev. D* **65**, 084003 (2002).
5. G. B. Cook and H. P. Pfeiffer, *Phys. Rev. D* **70**, 104016 (2004).
6. M. Caudill, G. B. Cook, J. D. Grigsby and H. P. Pfeiffer, *Phys. Rev. D* **74**, 064011 (2006).
7. A. Buonanno, G. B. Cook and F. Pretorius, *gr-qc/0610122* (2006).
8. H. P. Pfeiffer, D. A. Brown, L. E. Kidder, L. Lindblom, G. Lovelace and M. A. Scheel, *gr-qc/0702106* (2007).
9. S. Brandt and B. Brügmann, *Phys. Rev. Lett.* **78**, 3606 (1997).
10. H. P. Pfeiffer, L. E. Kidder, M. A. Scheel and S. A. Teukolsky, *Comput. Phys. Commun.* **152**, 253 (2003).
11. M. A. Scheel, H. P. Pfeiffer, L. Lindblom, L. E. Kidder, O. Rinne and S. A. Teukolsky, *Phys. Rev. D* **74**, 104006 (2006).
12. L. Lindblom, M. A. Scheel, L. E. Kidder, R. Owen and O. Rinne, *Class. Quantum Grav.* **23**, S447 (2006).